

贴体坐标系下求解复杂几何域内的单相流动

陈勇进¹, 陆慧林², 吴惠忠¹

(1. 上海·第七一研究所, 上海 200011; 2. 哈尔滨工业大学 能源学院, 黑龙江 哈尔滨 150001)

摘 要: 文中结合偏微分方程法生成的贴体坐标系统和 SIMPLEC 算法(协调一致的求解压力耦合的半隐算法), 将具有复杂几何形状的流动问题转换到可以应用有限差分法的计算平面进行数值模拟, 并对具有弯曲边界流道内的流动进行了预报, 讨论了流道形状对流动状况的影响。

关 键 词: 贴体坐标系; SIMPLEC 算法; 双方程紊流模型

中图分类号: O29; TB11 文献标识码: A

1 前言

有限差分方法作为一种成熟的数值方法积累了很多成功的算法, 而且具有计算稳定的特点^[1]。但是由于受到坐标系的束缚, 很难推广到复杂几何形状的流场中去。随着贴体网格技术的出现, 有限差分法得到了更为广泛的应用, 同时也给网格的生成方法提出了新的课题。本文试图利用流场边界节点疏密分布来控制内部节点的疏密安排, 简化贴体网格布局的过程, 以便快速获得具有较好的正交性和贴体性、疏密程度适合物理场变化的计算网格。同时, 由于现有的各种描述流动的数学模型, 尤其是工程应用中具有实际意义的湍流模型各有优劣, 与其说通过数值模拟找到一种适用于各种流动的数学模型不如说是在研究中确定这种模型的适用范围更好^[2]。因此流动的数值模拟还需要大量的比较工作, 本文选用了工程实际中应用较为广泛的双方程湍流模型, 并结合壁面函数法对几种复杂几何形状的管道内流动进行了数值模拟, 考察了方程对回流型管道内流动的模拟效果并给出了相关分析。

2 贴体网格的生成

$$\begin{aligned} d_{i+1} &= \sqrt{(x_{i+1} - x_i)^2 + (y_{i+1} - y_i)^2} & d_{j+1} &= \sqrt{(x_{j+1} - x_j)^2 + (y_{j+1} - y_j)^2} \\ d_{i-1} &= \sqrt{(x_i - x_{i-1})^2 + (y_i - y_{i-1})^2} & d_{j-1} &= \sqrt{(x_{j+1} - x_j)^2 + (y_{j+1} - y_j)^2} \\ d_i &= \sqrt{(x_{i+1} - x_{i-1})^2 + (y_{i+1} - y_{i-1})^2} & d_j &= \sqrt{(x_{j+1} - x_{j-1})^2 + (y_{j+1} - y_{j-1})^2} \end{aligned} \quad (3)$$

2.1 偏微分方程法生成贴体网格

贴体坐标的网格生成问题实际上是一个边值问题, 这就规定了变换函数必须是单值连续函数, 假设两套坐标系间存在以下的函数关系:

$$x = x(\xi, \eta), \quad y = y(\xi, \eta) \quad (1)$$

而满足 Laplace 方程和 Poisson 方程的调和函数具有上述特点, 所以贴体坐标系统的变换可以看作在给定边界条件下求解这一类椭圆型方程。由于是用数值方法求解, 微分方程法可以适用于各种复杂的几何形状, 使得网格生成程序具有通用性。

2.2 网格的疏密控制

在构造坐标转换函数过程中, 为了使物理平面上的网格划分能够适应物理场的变化, Thompson 通过在 Poisson 方程中添加源项控制网格的疏密程度^[1]。但是他推荐的源项形式复杂, 涉及到的经验系数很多, 不易掌握。事实上, 工程实际中大多数的设备外形是已知的, 如果事先确定好边界上节点疏密, 并将其反映到求解区域的内部就能够得到符合计算要求的贴体网格。由于微分方程的源项能够控制节点的分布, 反过来已知节点的分布情况也可以确定方程中源项的大小。所以, 只要计算出边界节点源项, 再通过插值得到两条边界线间内部节点的源项值, 就能在流场内部反映出边界节点的疏密。对于任意两条相邻的边界线 Γ_1, Γ_2 , 源项计算方法如下:

$$\Gamma_1: \begin{cases} P_i = \alpha_p \frac{1}{d_{i+1}} - \frac{1}{d_{i-1}} \\ Q_i = 0 \end{cases} \quad \Gamma_2: \begin{cases} P_i = 0 \\ Q_j = \alpha_q \frac{1}{d_{j+1}} - \frac{1}{d_{j-1}} \end{cases} \quad (2)$$

式中, α_p, α_q 是收缩因子, 用来根据计算的需要进一步调整内部网格节点位置, 通常情况下取 $\alpha_p = \alpha_q \approx$

2.0 即可满足要求, 函数 d 的取值方法如下:

除此之外, 可以利用边界节点分布生成函数和区域对接法等措施增加网格生成方法的通用性, 能够进一步方便地得到符合计算需要的、具有良好质量的贴体网格^[3]。图 1 中 (a) 和 (b) 的对比可以看出边界源项对网格疏密控制的效果, 内部节点的源项值采用线性插值。

3 贴体坐标系下流动控制方程及其离散

3.1 贴体坐标下流动控制方程的转换

$N-S$ 方程是描述流体运动的基本方程组, 人们通过将其中未知的切应力 $\tau_{i,j}$ 和可以用速度表示的假设变量关联起来, 进而采用数值方法对方程组求解。双方程模型就是其中的一种假设, 由于在方程组中引入了湍流动能 κ 和湍流耗散能 ϵ 来确定切应力, 每个控制单元里产生了影响流动的源项, 这可以理解为粘性切应力对流动的作用, 所以湍流的流动状态比层流复杂的多。根据数学分析理论, 不同的坐标系存在着函数关系, 可以通过坐标间的导数关系式来确定控制方程中物理变量 Φ 在转换过程中产生的协变量。整理后得到流动控制方程的通用形式如下:

$$\frac{1}{J} \frac{\partial}{\partial \xi} (\rho U \Phi) + \frac{1}{J} \frac{\partial}{\partial \eta} (\rho V \Phi) = \frac{1}{J} \frac{\partial}{\partial \xi}$$

$$\left[\frac{\Gamma}{J} (\alpha \Phi_{\xi} - \beta \Phi_{\eta}) \right] + \frac{1}{J} \frac{\partial}{\partial \eta} \left[\frac{\Gamma}{J} (-\beta \Phi_{\xi} + \gamma \Phi_{\eta}) \right] + S(\xi, \eta) \quad (3)$$

其中, α, β, γ, J 是坐标系间的导数关系式, U, V 是受到协变量影响的物理变量的新组合。表 1 是控制方程源项 $S(\xi, \eta)$ 的展开表达形式。

3.2 数学方程的离散及计算

应用有限差分法离散贴体坐标系下的流动控制方程时, 每一个节点上的变量变化不仅受到近邻的四个节点的影响, 交叉方向上的四个远邻点产生的协变量也要考虑, 这样就使五点格式的离散方程变为九点格式的代数方程, 所求解的变量数增加了一倍, 但将其整理归并后, 得到的离散方程仍显示物理平面上控制方程具有的特性, 所以各种在矩形或其他规则计算区域内开发出来的算法都可以推广到贴体坐标的计算平面中去。本文利用压力修正的 SIMPLEC 算法求解物理平面上各种复杂几何域内的

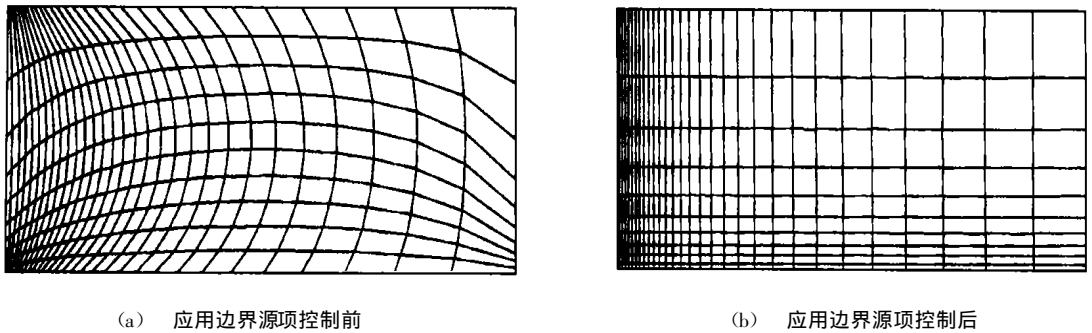


图 1

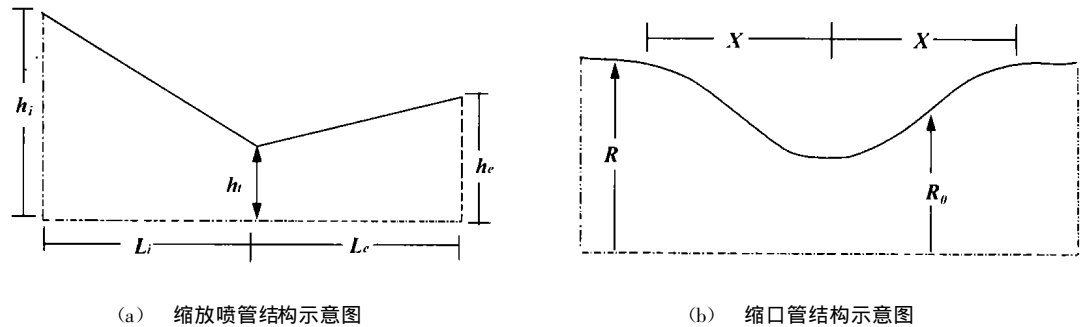


图 2

流动问题, 用混合差分离散方程中的对流项, 中心差分离散源项和扩散项, 交替线迭代法 (ADI) 求解离散得到的五对角代数方程组, 最后采用交错网格抑制可能出现的锯齿形压力场。

4 计算结果与分析

本文作者对具有复杂几何形状的缩放喷管和缩口管进行了数值模拟, 为了将本文的模拟结果和相关文献的实验数据进行比较, 模拟对象的结构分别采用了 Mabson 所做的二维缩放喷管实验^[4] 以及 Deshpande 和 Giddens 的轴对称缩口管试验^[5], 图 2 计算区域的结构示意图。

表1 贴体坐标系下流动控制方程中源项展开表达式

物理平面内源项		计算平面内源项	
S_u	$\frac{\partial}{\partial x}(\mu_{eff} \frac{\partial u}{\partial x}) + \frac{\partial}{\partial y}(\mu_{eff} \frac{\partial v}{\partial x})$	$\frac{1}{J} \{ [\frac{\mu_{eff}}{J} (U_{\xi y \eta} - U_{\eta y \xi})] \xi + [\frac{\mu_{eff}}{J} (V_{\xi y \eta} - V_{\eta y \xi})] \eta \}$	
S_v	$\frac{\partial}{\partial x}(\mu_{eff} \frac{\partial u}{\partial y}) + \frac{\partial}{\partial y}(\mu_{eff} \frac{\partial v}{\partial y})$	$\frac{1}{J} \{ [\frac{\mu_{eff}}{J} (-U_{\xi x \eta} + U_{\eta x \xi})] \xi + [\frac{\mu_{eff}}{J} (-V_{\xi x \eta} + V_{\eta x \xi})] \eta \}$	
S_k	$G - \rho \epsilon$	$G - \rho \epsilon$	
S_ϵ	$\frac{\epsilon}{K} (c_1 G - c_2 \rho \epsilon)$	$\frac{\epsilon}{K} (c_1 G - c_2 \rho \epsilon)$	
G	$\mu_t \{ 2 [(\frac{\partial u}{\partial x})^2 + (\frac{\partial v}{\partial y})^2] + (\frac{\partial u}{\partial y} + \frac{\partial v}{\partial x})^2 \}$	$\frac{\mu_t}{J^2} \{ 2 [(u_{\xi y \eta} - u_{\eta y \xi})^2 + (-v_{\xi x \eta} + v_{\eta x \xi})^2] + (-u_{\xi x \eta} + u_{\eta x \xi} + v_{\xi y \eta} - v_{\eta y \xi})^2 \}$	

$\mu_{eff} = \mu_t + \mu$

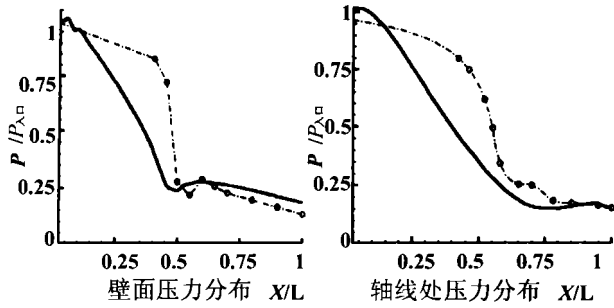


图3 缩放喷管壁面和轴线处压力分布

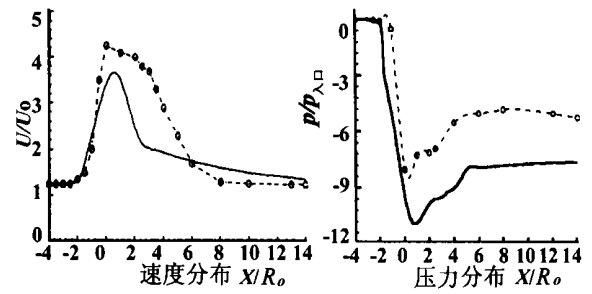


图4 缩口管速度和压力分布

缩放喷管中共布置了 81×21 个网格节点, 纵轴方向上网格节距均匀划分, 横轴方向上网格点向喷管喉部密集。入口流速是 0.232 马赫数, 入口静压已知。轴对称收缩管中布置了 52×12 个网格节点, 纵向上网格等距, 轴向上网格向通道直径最小处集中。在这一例 $Re = 1.5 \times 10^4$ 的紊流流动实验中, x 方向上计算区域的长度取为 $-4R_0 < x < 14R_0$, 入口条件根据 Deshpande 和 Giddens 总结实验数据获得的经验公式取值^[3]。

图3显示的是缩放喷管中心线和壁面上沿横轴压力变化的曲线图。图4是缩口管轴对称线上速度和

壁上压力分布的曲线图, 图中实线代表计算值, 圆点代表实测值, 节点线是由实测值拟和的曲线。从两例具有倾斜或弯曲边界的通道中的流场模拟和

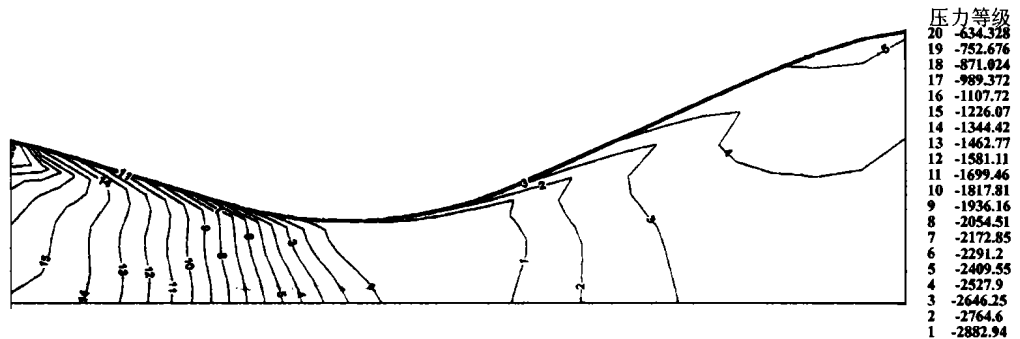


图5(a)喷管A的压力等势剖面

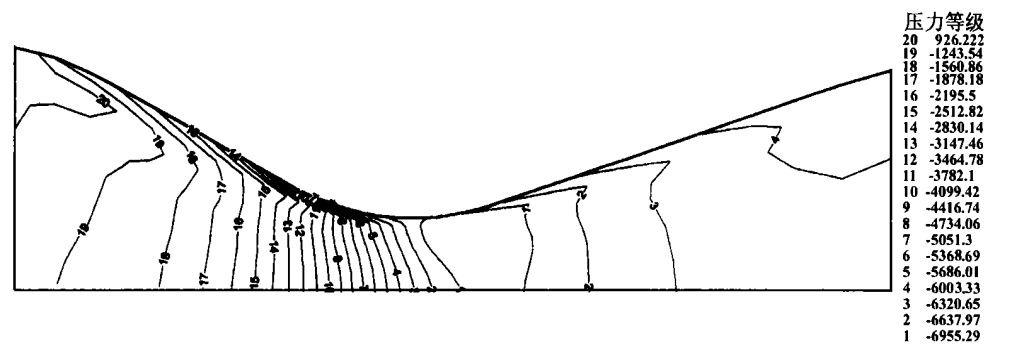


图5(b)喷管B的压力等势剖面

实验结果的比较来看, 各种变量在径向和轴向的变化趋势基本吻合, 证明模拟是成功的。由于双方程模型和壁面函数法在模拟湍流流动时都作了假设, 而缩口管的弯曲边界比缩放喷管中倾斜边界更接近于假设所需要的条件, 图 4 中缩口管收缩段的模拟值和实验几乎完全重合, 可以认为在通道界面剧烈变化区域, 湍流特性系数各向异性强烈, 壁面函数法的假设已不能成立, 通道喉部模拟计算值和实验数据存在偏差, 需要引入更为恰当模型, 低雷诺模型是可以考虑的一个替代手段。

图 5 是两例出入口带收敛弧段、喉部由圆弧过渡的缩放喷管内流动的数值模拟效果图。从中我们能够直观地看到流体在喷管中压力的变化, 从压力等势图可以看出, 由于壁面对流体的滞止作用, 流速在靠近壁面处陡然下降, 流体减速增压, 但由于摩擦引起的内能损失使流体很快过渡到总体的速度和压力同时下降。A 型喷管出口处的壁面压力曲线几乎封闭, 说明此时流体和壁面出现了分离, 增大了流动损失, 因此采用有较大收缩比的 B 型喷管可以降低湍流度、减薄边界层, 提高流动效率。

5 结论

(1) 椭圆型偏微分方程固有的光滑边界数据的特性使得生成的网格具有较好的正交性, 利于数值

计算的收敛, 利用边界节点疏密分布实现复杂边界内网格分布的疏密控制方法简便、通用性强, 易于网格的主动设计。

(2) 贴体坐标系统将流动问题从复杂的物理平面转移到简单而易于处理的计算平面也付出了一定的代价, 计算平面上控制方程的复杂化带来了计算量的增加, 但计算机性能的提高和高效解法的出现使得这一问题并不突出, 而有限差分算法的稳定性和差分格式的多样化十分有利于数值模拟的成功。

(3) $k-\epsilon$ 湍流模型和壁函数法构建的数学模型基本反映了弯曲边界通道内亚音速流动的实际情况, 在此基础上开发的程序具有实用性。

参考文献:

- [1] 陶文铨. 数值传热学[M]. 西安: 西安交通大学出版社, 1989.
- [2] 周力行. 湍流两相流动与燃烧的数值模拟[M]. 北京: 清华大学出版社, 1991.
- [3] 方丁酉. 两相流体动力学[M]. 北京: 科学技术出版社, 1984.
- [4] KORBI K C, PATANDAR S V. Pressure based calculation procedure for viscous flows at all speed in arbitrary contiguation[J]. *AIAA*, 1989, 27(9): 1167—1174.
- [5] MELAAEN M C. Analysis of fluid flow in constricted tubes and ducts using body-fitted non-staggered grids[J]. *Int J Numer Methods Fluids*, 1991, 15(2): 895—923.
- [9] CHEN LINGEN, SUN FENGRUI, WU CHIH. Effect of heat transfer law on the performance of a generalized irreversible Camot engine[J]. *J Phys D App Phys*, 1999, 32(2): 99—105.
- [10] CHEN LINGEN, SUN FENGRUI, WU CHIH. Influence of heat transfer law on the performance of a Camot engine[J]. *App Thermal Engineering*, 1997, 17(3): 277—282.
- [11] GORDON JM, HULEIHIL M. General performance characteristics of real heat engines[J]. *J App Phys*, 1992, 72(2): 829—837.
- [12] CHEN LINGEN, SUN FENGRUI, WU CHIH. Performance analysis of an irreversible Brayton heat engine[J]. *J Intuit Energy*, 1997, 70(482): 2—8.
- [13] FEIDT F. Optimization of Brayton cycle engine in contact with fluid thermal capacities[J]. *Rev Gen Term*, 1996, 35(10): 662—666.
- [14] O SULLIVAN C T. Newton's law of cooling—A critical assessment [J]. *Am J Phys*, 1990, 58(10): 956—960.

(渠 源 编辑)

(渠 源 编辑)

(上接第 175 页)

- [3] WU CHIH, CHEN LINGEN, CHEN JINCAN. Recent Advances in Finite-Time Thermodynamics[M]. New York: Nova Science Publishers, 1999.
- [4] BEJAN A. Entropy Generation Minimization[M]. Boca Raton: CRC Press, 1996.
- [5] CHEN LINGEN, WU CHIH, SUN FENGRUI. The influence of internal heat leak on the power versus efficiency characteristics of heat engines[J]. *Energy Converse*, 1997, 38(4): 1501—1507.
- [6] WU C, KIANG R L. Finite-time thermodynamic analysis of a Camot engine with internal irreversibility[J]. *Energy*, 1992, 17(12): 1173—1178.
- [7] 陈林根, 孙丰瑞. 不可逆卡诺热机的性能[J]. *科技通报*, 1995, 11(2): 128.
- [8] CHEN LINGEN, WU CHIH, SUN FENGRUI. A generalized model of real heat engines and its performance[J]. *J Insitute energy*, 1996, 69(481): 241—222.

burning test rig. The measuring and test results are presented. **Key words:** charge-coupled device, temperature measurement, genetic algorithm

基于火焰图像处理的炉膛辐射能信号的检测及分析= **Flame Image Processing-based Detection and Analysis of Furnace Radiation Energy Signals** [刊, 汉] / ZHANG Shi-shuai, ZHOU Huai-chun (Power Engineering Department, Huazhong University of Science & Technology, Wuhan, China, Post Code: 430074), PENG Min, LIU Wu-lin (Central Testing Institute under the Hunan Provincial Electric Power Bureau, Changsha, China, Post Code: 410007) // Journal of Engineering for Thermal Energy & Power. — 2002, 17(2). — 166 ~ 168, 182

An on-site detection test was conducted on a 300 MW coal-fired boiler of Xiangtan Power Plant by the use of a flame image processing-based detection system of furnace radiation-energy signals. In addition, an analysis has been performed on the relationship between the furnace radiation energy signals and the boiler main operating parameters. The results of the analysis indicate that the furnace radiation energy signals can to a certain extent not only forecast the actual output of the boiler, but also reflect the combustion conditions in the boiler. **Key words:** coal-fired boiler, flame image, furnace radiation energy, detection method

六角燃烧锅炉同心双切圆流场的数值模拟研究= **Numerical Simulation Study of the Concentric Double-tangential Circular Flow Field of a Hexagonal-fired Boiler** [刊, 汉] / ZHAO Yu-xiao, LI Rui-yang, WANG Shi-jun, QIN Yu-kun (Energy Source College under the Harbin Institute of Technology, Harbin, China, Post Code: 150001), LU Wei (Thermal Energy Engineering Department, Harbin University of Science & Technology, Harbin, China, Post Code: 150040) // Journal of Engineering for Thermal Energy & Power. — 2002, 17(2). — 169 ~ 171

By the use of a $k-\epsilon$ dual-equation turbulent flow model and a particle random trajectory model a numerical simulation is conducted of the burner-zone flow field of a boiler, which adopts wall-installed burners. The primary and secondary air jet flow of the upper layer burner has been arranged in the form of a concentric dual-tangential circle. Through an analysis of the variation of flow field characteristics the cause of slag formation on prototype heating surfaces is investigated and a method for resolving the issue sought out. **Key words:** $k-\epsilon$ dual equation turbulent flow model, particle random trajectory model, concentric dual-tangential circle

导热规律服从 $q \propto (\Delta T)^n$ 广义不可逆卡诺热机的最优性能= **Optimal Performance of a Generalized Irreversible Carnot Engine with Heat Conduction Law Subordinate to $Q^{\mu}(DT)^n$** [刊, 汉] / ZHOU Sheng-bing, CHEN Lin-gen, SUN Feng-rui (No. 306 Teaching and Research Department under the Naval Engineering University, Wuhan, China, Post Code: 430033) // Journal of Engineering for Thermal Energy & Power. — 2002, 17(2). — 172 ~ 175, 179

Taking into account the thermal resistance losses between a working medium and heat source a constant term is used to express heat leakage loss and a constant factor term to express other irreversible items in a cycle plant with the exception of the heat resistance and heat leakage. As a result, set up is an irreversible Carnot engine model. On the basis of another kind of relatively universal heat conduction law, i. e., $Q^{\mu}(DT)^n$ derived is the optimal characteristic relationship between the heat engine power and efficiency. Through detailed numerical calculations an analysis is performed of the effect on the optimal performance of a generalized irreversible heat engine by the heat leakage, internal irreversibility and heat conduction law. **Key words:** finite-time thermodynamics, heat engine, performance optimization

贴体坐标系下求解复杂几何域内的单相流动= **The Solution of a Single-Phase Flow in a Complicated Geomet-**

ric Domain under an Adherent Body Coordinate System [刊, 汉] / CHEN Yong-jin, WU Wei-zhong (No. 711 Research Institute, Shanghai, China, Post Code: 200090), LU Wei-lin (Energy Source College under the Harbin Institute of Technology, Harbin, China, Post Code: 150001) // Journal of Engineering for Thermal Energy & Power. — 2002, 17(2). — 176 ~ 179

In conjunction with an adherent body coordinate system generated by a partial differential equation method and a SIMPLEC algorithm (a half-hidden algorithm for a coordinated solution of pressure coupling) a flow problem with a complicated geometric shape is converted to a calculation plane. For the latter a numerical simulation can be conducted by the use of a finite difference method. Furthermore, the flow in a flow duct with a curved boundary is forecast along with a discussion of the effect of flow duct shape on flow conditions. **Key words:** adherent body coordinate system, SIMPLEC algorithm, dual equation turbulent flow model

电站锅炉天然气点火装置的设计与研究 = Design and Study of the Natural Gas Ignition Device of a Utility Boiler [刊, 汉] / LIU Sheng-yong, ZHANG Bai-liang (Key Lab of Renewable Energy Under the Ministry of Agriculture, Zhengzhou, China, Post Code: 450002), LIU Zhi-gang (Xi'an Jiaotong University Xi'an, China, Post Code: 710049), WANG Jin-tao (Dengfeng Power Plant, Zhengzhou, China, Post Code: 450000) // Journal of Engineering for Thermal Energy & Power. — 2002, 17(2). — 180 ~ 182

All utility boilers in China use oil for ignition and combustion-support with oil consumption in this regard hitting more than 400, 000 tons each year. The substitution of oil by coal has become an issue demanding an urgent solution. Based on the characteristics of natural gas the authors have by adopting a forced pre-mix combustion mode designed for an ignition device spray nozzles and an ejector, and conducted a study on the method of achieving flame stabilization. Under the condition of a given air-fuel ratio a test was conducted to identify the relationship between natural gas flow rate and ignition parameters. As a result, the optimum flow rate of the natural gas has been found to be $0.00172 \text{ m}^3/\text{s}$ with the flame temperature being as high as 1820°C and flame length 1.11 m. The use of the ignition device shows that it has the following merits: a high flame temperature, strong adaptation ability and ease of operation, etc. As compared with the former oil-ignition device, the pre-burning time of the natural gas ignition device is 1/4 of that of the oil ignition one while the cost is only 1/800 of the latter. **Key words:** utility boiler, natural gas, ignition device

某船主锅炉的设计特点 = Design Features of a Marine Main Boiler [刊, 汉] / CHEN Ming, MA Yun-xiang, XUE Guang-ya, CHEN Qi-duo (Harbin No. 703 Research Institute, Harbin, China, Post Code: 150036) // Journal of Engineering for Thermal Energy & Power. — 2002, 17(2). — 183 ~ 185, 210

A new type of marine main boiler designed by Chinese engineers was put into operation. It features a new construction, new materials and technologies. The structural design of this type of boiler is presented along with a description of its performance characteristics. **Key words:** marine main boiler, structural design, performance features

湿法脱硫除尘一体化装置应用中的问题及解决措施 = Some Problems Concerning the Use of an Integrated Wet Desulfurization and Dust Separation Device as well as Measures Taken for their Resolution [刊, 汉] / ZHAO Xu-dong, WU Shao-hua (Energy Science and Engineering College under the Institute of Technology, Harbin, China, Post Code: 150001), MA Chun-yuan, et al (Power Engineering Department, Shandong University, Jinan, China, Post Code: 250000) // Journal of Engineering for Thermal Energy & Power. — 2002, 17(2). — 186 ~ 188

From the aspects of the operating parameters of a wet desulfurization system and its system configuration expounded are the existing problems involved in the industrial operation of an integrated wet desulfurization and dust-separation device.